

Clustering of spectra and fractals of regular graphs

V. Ejov¹, J.A. Filar¹, S.K. Lucas², P. Zograf³

¹ School of Mathematics and Statistics, University of South Australia,
Mawson Lakes SA 5095 AUSTRALIA

² Department of Mathematics and Statistics, James Madison University,
Harrisonburg, VA 22807, USA

³ St. Petersburg Department of Steklov Institute of Mathematics,
Fontanka 27, St.Petersburg 191023 RUSSIA

Abstract. We exhibit a characteristic structure of the class of all regular graphs of degree d that stems from the spectra of their adjacency matrices. The structure has a fractal threadlike appearance. Points with coordinates given by the mean and variance of the exponentials of graph eigenvalues cluster around a line segment that we call a *filar*. Zooming-in reveals that this cluster splits into smaller segments (filars) labeled by the number of triangles in graphs. Further zooming-in shows that the smaller filars split into subfilars labelled by the number of quadrangles in graphs, etc. We call this fractal structure, discovered in a numerical experiment, a *multifilar structure*. We also provide a mathematical explanation of this phenomenon based on the Ihara-Selberg trace formula, and compute the coordinates and slopes of all filars in terms of Bessel functions of the first kind.

Key words. Regular graph, spectrum, fractal, Ihara-Selberg trace formula

1. A numerical experiment

For the sake of simplicity we will pay our attention mainly to cubic graphs (or, in other words, to regular graphs of degree $d = 3$). This assumption is not restrictive since all our considerations remain valid for regular graphs of degree $d > 3$ with obvious minor modifications. Moreover, in a certain sense cubic graphs are the generic regular graphs (see e.g. Greenlaw and Petreschi [3])¹.

So let us consider the set of all regular cubic graphs with n vertices. They can be conveniently enumerated using the GENREG program of Markus Meringer [6]. Each graph is completely determined by its adjacency matrix, which is symmetric. Its spectrum (the set of eigenvalues) is real and lies on the segment $[-3, 3]$. For each graph it can be found numerically. In the interests of statistical analysis, we might want to take the means and variances of each set of eigenvalues. However, since the diagonal entries of the adjacency matrices are zero (graphs contain no loops), the eigenvalues sum to zero. In order to produce results with some variation, and originally motivated by solving systems of linear first order differential equations, we take the exponential of the eigenvalues before finding their mean and variance. As a final modification, this time motivated by the authors'

¹ Actually, cubic graphs are generic in a wider sense: *any* graph can be made cubic by a small perturbation that blows up vertices into small circles.

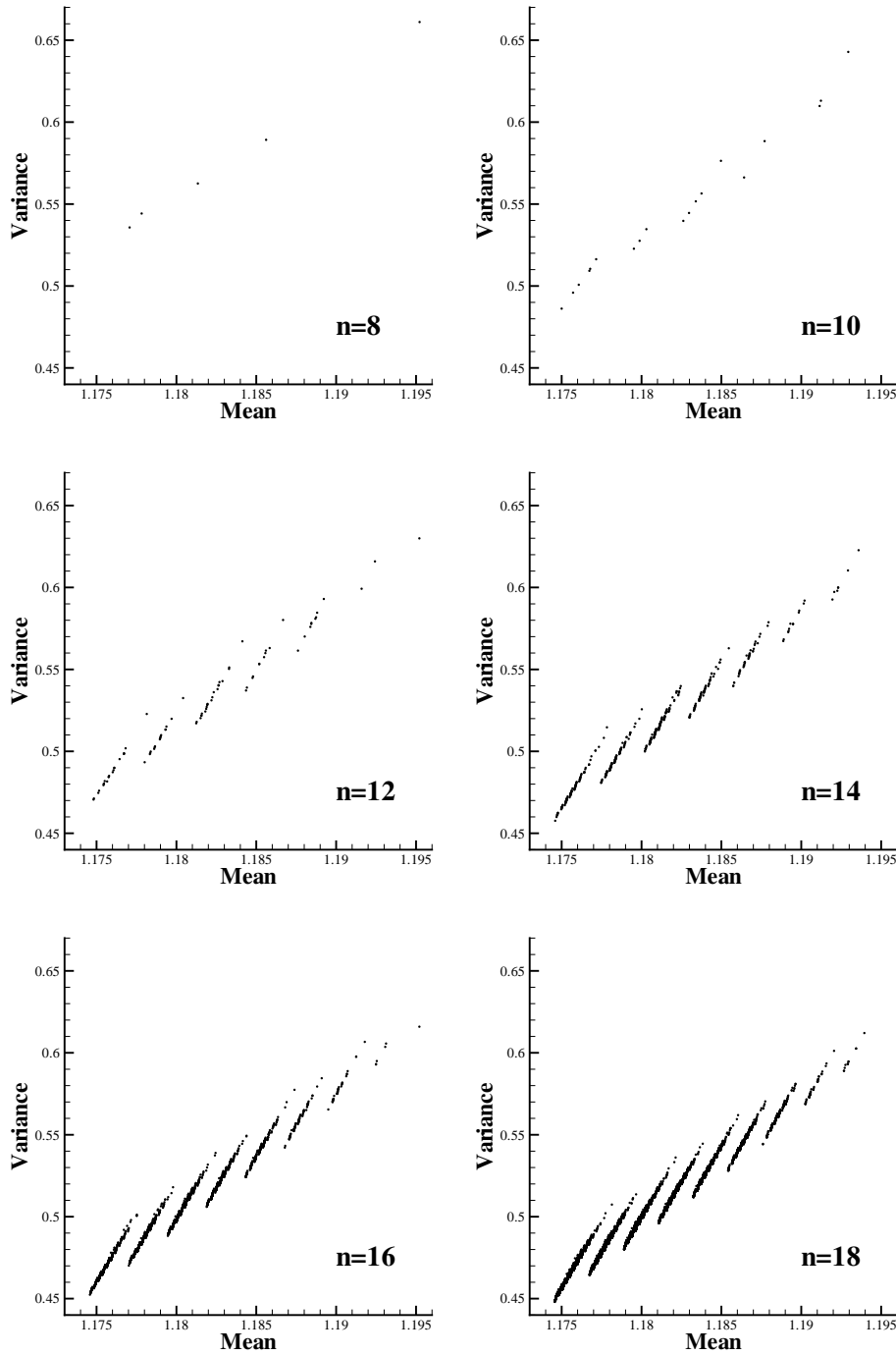


Fig. 1. Plots of mean versus variance for the exponential of the eigenvalues of the doubly stochastic matrices associated with all regular cubic graphs with various numbers of vertices.

interest in Markov processes, we replace the adjacency matrix A by the related doubly stochastic matrix $\frac{1}{3}A$. The theory of Markov chains then states that the probability of being at the j th vertex after a walk of length i in the graph with each edge equally likely to be chosen is the j th element of the vector $(\frac{1}{3}A)^i \mathbf{x}$, where the k th element of the vector \mathbf{x} is the probability of starting at the k th vertex.

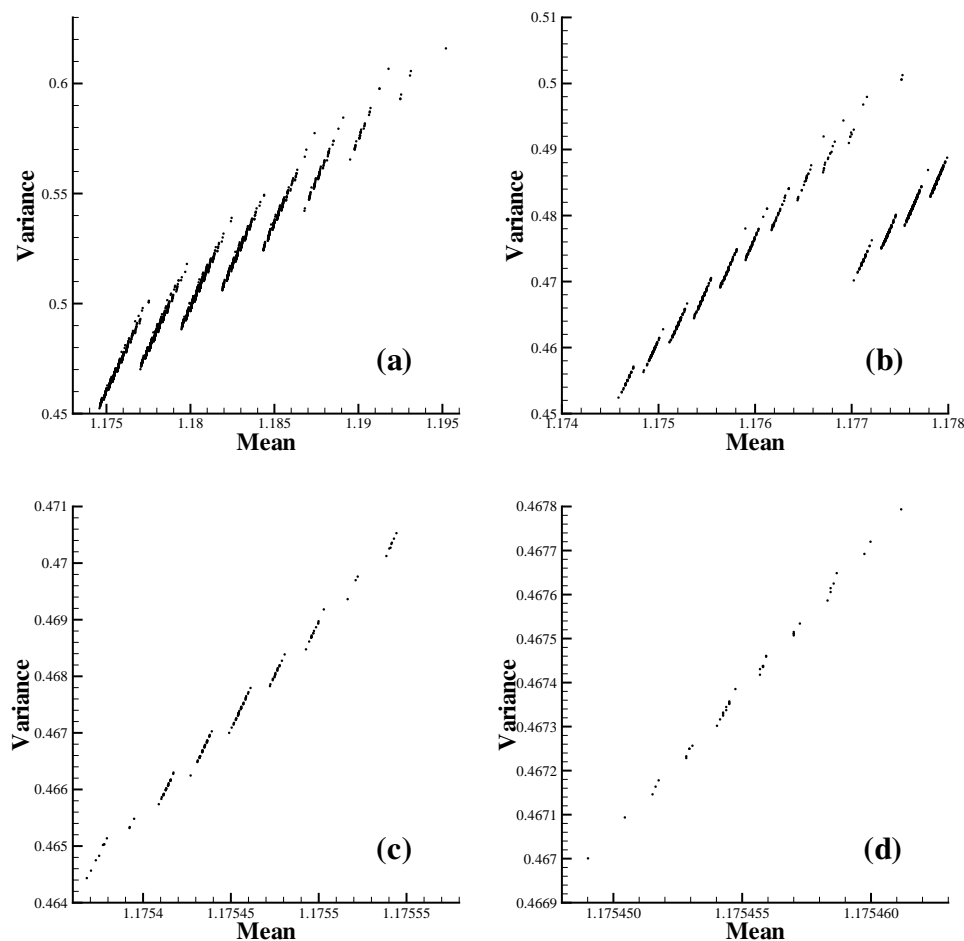


Fig. 2. Successively zooming in on the $n = 14$ plot

Summarizing, we apply the following procedure. For a fixed even n find the adjacency matrices of all regular cubic graphs on n vertices. In each case, divide the adjacency matrix by three, find its eigenvalues, take their exponential, and then find their mean and variance. Each cubic graph is then represented by a single dot on a plot of mean versus variance. Figure 1 shows the results of applying this procedure with $n = 8, 10, 12, 14, 16, 18$, where the number of regular cubic graphs in each case is 5, 19, 85, 509, 4060, 41301 respectively. There appears to be a very definite structure in these plots. In each case the data appear in distinct clusters that at this scale look like straight line segments with roughly the same slope and distance separating them. (In the next section we will derive explicit formulas for these slopes and distances.) Due to their form, we would like to name these clusters by “filars”, whose dictionary meaning is “threadlike objects”².

An even greater level of structure exists within each filar. Figure 2(a) repeats the results for $n = 16$, and Figure 2(b) zooms in on the leftmost filar. We can see that each filar is in fact made up of smaller clusters of approximately straight line segments, all roughly parallel and the same distance apart, with a steeper slope than the original one. We shall call each of these clusters a subfilar, and Figure 2(c) zooms in on the fourth subfilar from the left in Figure 2(b). The structure continues in Figure 2(d), which zooms in on the

² This term also recognizes the second author’s (JF’s) initial investigation of the above phenomenon.

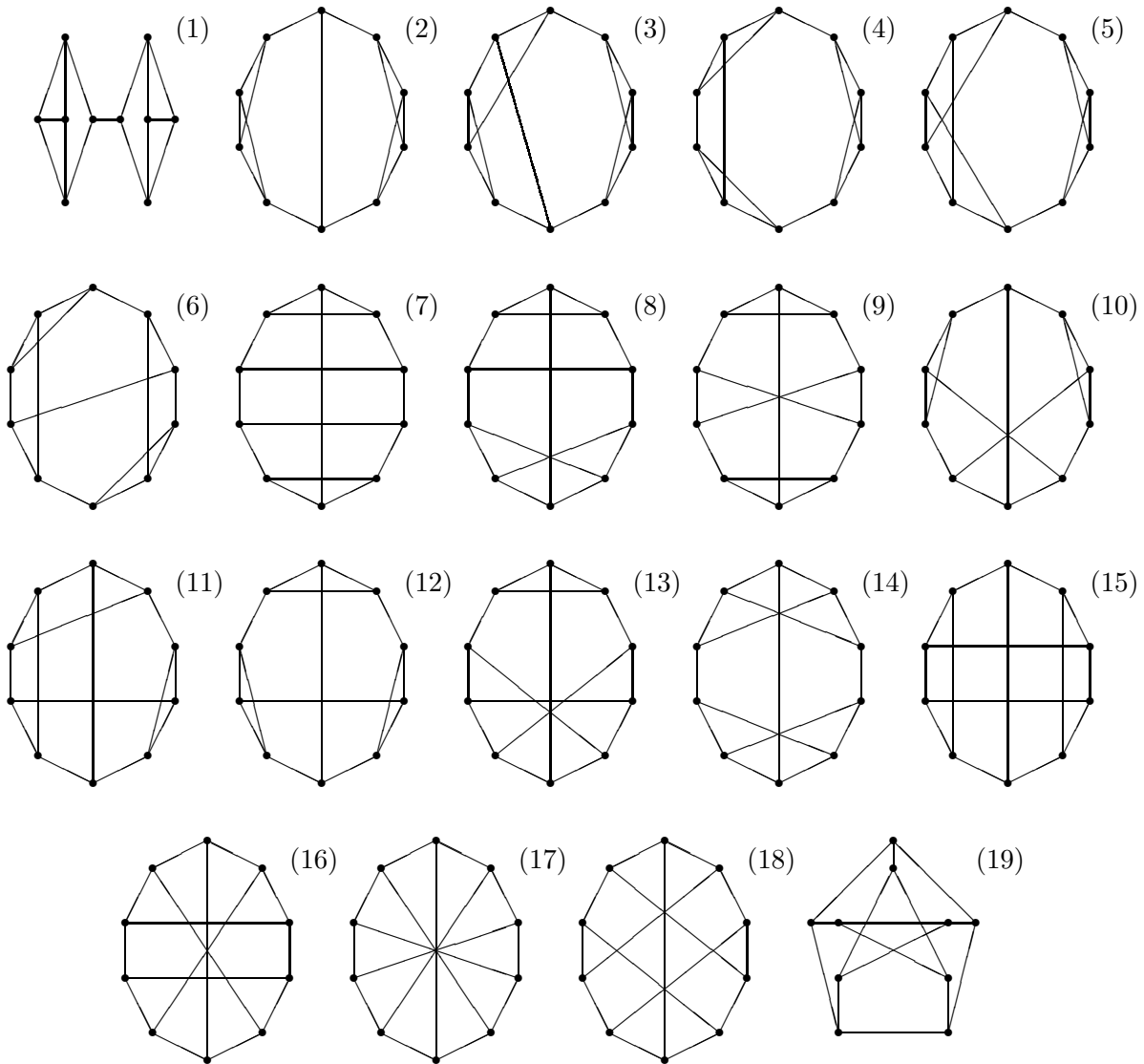


Fig. 3. All cubic graphs with ten vertices, as output by GENREG

5th subsubfilar of Figure 2(c). Since a fractal is defined as a self-similar image, where the same structure is evident when magnifying one part of the image, we see that these figures obviously enjoy a fractal structure. The larger the number of vertices, the more levels of magnification can be undertaken before the number of data points becomes small enough for the self-similar structure to be lost. Collectively, we refer to this phenomenon as the “multifilar structure” of cubic graphs (or their spectra, to be more precise).

Finally, it is worth noting that this behavior is not limited to cubic graphs. Plots for quartic graphs (every vertex of degree four) show exactly the same structure. As we will see later, the Ihara-Selberg trace formula justifies the presence of such a fractal structure for regular graphs of arbitrary degree d .

Having – to the best of our knowledge – for the first time discovered this property of regular graphs, the aim of the following section is to theoretically explain the (multi)filar structure.

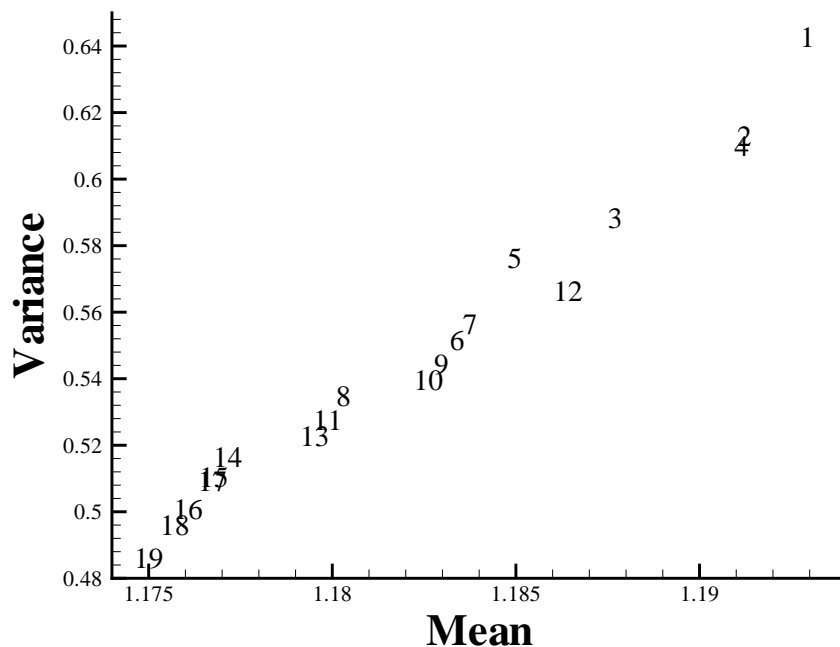


Fig. 4. A reproduction of Figure 1 ($n = 10$) with labels replacing data points related to associated with graphs in Figure 3

2. Theoretical justification

2.1. Ten vertex cubic graphs in detail

Before we resort to the theory based on the Ihara-Selberg trace formula [4,1], it is instructive to consider the case $n = 10$ in detail. Figure 3 shows all 19 regular cubic graphs with ten vertices, labelled in the order produced by GENREG, and Figure 4 repeats Figure 1(b), but with labels on the data points indicating graph number. We can see a pattern in terms of which graphs are in each filar. Graphs 19,18,16,17,15,14 in the first (leftmost) filar have no subcycles of length 3, which we shall call triangles from now on. Graphs 13,11,8 in the second filar have exactly one triangle, graphs 10,9,6,7,5 in the third filar have exactly two triangles, graphs 12,3 in the fourth filar have exactly three triangles, and graphs 4,2,1 in the fifth filar have exactly four triangles. Focusing on the first filar, graphs 19,18,16,17,15,14 have exactly 0,2,3,5,5,6 subcycles of length 4 respectively. Special emphasis should be given to the data points for graphs 17 and 15. They are extremely close together, and have the same number of subcycles of lengths 3 and 4 (0 and 5 respectively). They only vary in number of subcycles of length 5, numbering 0 and 2. Similarly, graphs 4 and 2 both have four 3-subcycles, two 4-subcycles, and only vary in the number of 5-subcycles (two and four). These observations suggest that membership in a filar structure is related to the number of subcycles of various lengths in the original graph – although this does not explain why filars approximate straight lines.

2.2. Explicit formulas for the mean and variance

To obtain qualitative and quantitative justification of the phenomenon in question we bring in a very explicit version of the Ihara-Selberg trace formula that is due to P. Mnëv, cf. [7], Formula (30). A general form of the Ihara-Selberg trace formula, as well as precise definitions can be found in Appendix. For any regular graph G of degree $d = q + 1$ on n vertices we have

$$\frac{1}{n} \sum_{i=1}^n e^{t\lambda_i} = \frac{q+1}{2\pi} \int_{-2\sqrt{q}}^{2\sqrt{q}} e^{st} \frac{\sqrt{4q-s^2}}{(q+1)^2-s^2} ds + \frac{1}{n} \sum_{\gamma} \sum_{k=1}^{\infty} \frac{\ell(\gamma)}{2^{k\ell(\gamma)/2}} I_{k\ell(\gamma)}(2\sqrt{q}t). \quad (1)$$

Here $\{\lambda_1, \dots, \lambda_n\}$ is the spectrum of the adjacency matrix of G , γ runs over the set of all (oriented) primitive closed geodesics³ in G , $\ell(\gamma)$ is the length of γ , and $I_m(z)$ is the standard notation for the Bessel function of the first kind:

$$I_m(z) = \sum_{r=0}^{\infty} \frac{(z/2)^{n+2r}}{r!(n+r)!}.$$

All lengths $\ell(\gamma)$ are integers greater than or equal to 3. Let us denote by m_ℓ the number of *non-oriented* primitive closed geodesics of length ℓ in the graph G . The numbers m_ℓ are called the *multiplicities* of the *length spectrum* of the graph G , that is, the set of lengths of non-oriented primitive closed geodesics in G (the set $\{m_3, m_4, \dots\}$ describes the length spectrum of the graph in a unique and convenient way). The multiplicities m_i are uniquely determined by the eigenvalues of G and are given by explicit formulas (cf. Formula (34) in [7])⁴. For instance, we have

$$n_3 = \frac{1}{6} \sum_{i=1}^n \lambda_i^3, \quad n_4 = \frac{1}{8} \left(\sum_{i=1}^n \lambda_i^4 - n(q+1)(2q+1) \right),$$

etc.

Now we rewrite Formula (1) in terms of the multiplicities n_ℓ (since we consider in detail only the case of cubic graphs, we also put $q = 2$):

$$\frac{1}{n} \sum_{i=1}^n e^{t\lambda_i} = J(t) + \frac{2}{n} \sum_{\ell=3}^{\infty} \ell m_\ell F_\ell(t), \quad (2)$$

where

$$J(t) = \frac{3}{2\pi} \int_{-2\sqrt{2}}^{2\sqrt{2}} e^{st} \frac{\sqrt{8-s^2}}{9-s^2} ds,$$

and

³ In the context of graphs, a *closed geodesic* is an oriented closed path of minimal length in its free homotopy class. A closed geodesic is called *primitive* if it is not a multiple of a shorter geodesic. Closed geodesics of length 3, 4 and 5 are 3-, 4- and 5-cycles in graphs respectively, whereas closed geodesics of length greater than 5 may have self-intersections. See Appendix for details.

⁴ Clearly, the length spectrum also determines the eigenvalue spectrum uniquely.

$$F_\ell(t) = \sum_{k=1}^{\infty} \frac{I_{k\ell}(2\sqrt{2}t)}{2^{k\ell/2}}.$$

Note that the factor of 2 at the sum appears because we forget about the orientation of geodesics and have to count each one of them twice. The latter series converges very fast because of the following well-known asymptotic behavior of $I_m(z)$:

$$I_m(z) \approx \frac{1}{m!} \left(\frac{z}{2}\right)^m \quad (3)$$

as $m \rightarrow \infty$ and $0 < z \ll \sqrt{m+1}$; see e.g. [9].

The closed form expressions for the mean μ and the variance σ can now be easily extracted from (2). Precisely, we have

$$\mu = \frac{1}{n} \sum_{i=1}^n e^{\lambda_i/3} = J(1/3) + \frac{2}{n} \sum_{\ell=3}^{\infty} \ell m_\ell F_\ell(1/3), \quad (4)$$

and⁵

$$\begin{aligned} \sigma &= \frac{1}{n} \sum_{i=1}^n \left(e^{\frac{\lambda_i}{3}} - \mu\right)^2 = \frac{1}{n} \sum_{i=1}^n \left(e^{\frac{2\lambda_i}{3}}\right) - \mu^2 \\ &= J(2/3) + \frac{2}{n} \sum_{\ell=3}^{\infty} \ell n_\ell F_\ell(2/3) - \mu^2. \end{aligned} \quad (5)$$

Substituting (4) into the last formula and neglecting quadratic terms in F_ℓ that are small in view of (3), we get

$$\sigma \approx (J(2/3) - J(1/3)^2) + \frac{2}{n} \sum_{\ell=1}^n \ell m_\ell (F_\ell(2/3) - 2J(1/3)F_\ell(1/3)). \quad (6)$$

Now we are set for explicitly describing the positions of filars.

2.3. Coordinates and slopes of filars

To start with, let us note that the function $F_\ell(t)$ is positive for $t > 0$ and decreases very rapidly when ℓ grows and t remains fixed. It is easy to check that $F_\ell(2/3) - 2J(1/3)F_\ell(1/3)$ is also positive for any positive integer $\ell \geq 3$ and decreases very fast in ℓ . Therefore, for any n all the points with coordinates (μ, σ) , corresponding to cubic graphs on n vertices, lie above and to the right of the initial point $(J(1/3), J(2/3) - J(1/3)^2) \approx (1.17455, 0.4217)$ in the mean vs. variance plane. Moreover, we see that $\ell = 3$ gives the leading terms in both sums in (4) and (6). This means that the points (μ, σ) accumulate just above the line parametrically described by equations

$$x = J(1/3) + tF_3(1/3) \approx 1.17455 + 0.00653t,$$

$$y = (J(2/3) - J(1/3)^2) + t(F_3(2/3) - 2J(1/3)F_3(1/3)) \approx 0.4217 + 0.0462t,$$

⁵ It should be mentioned that the plots on Figures 1 and 2 are build using the *unbiased* variance $s_{n-1}^2 = \frac{1}{n-1} \sum_{i=1}^n \left(e^{\frac{\lambda_i}{3}} - \mu\right)^2$. In order to make formulas simpler, we consider here the variance $s_n^2 = \frac{1}{n} \sum_{i=1}^n \left(e^{\frac{\lambda_i}{3}} - \mu\right)^2$. The difference is insignificant, especially for large enough n .

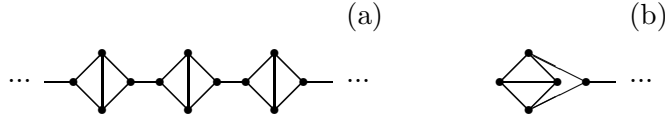


Fig. 5. A string of diamonds (a) and a clasp (b)

where x is the mean and y is the variance coordinates respectively. Note that the slope of this line is approximately 7.079.

Another byproduct of the above considerations is a necessary and sufficient condition for two graphs $G^{(1)}$ and $G^{(2)}$ to belong to the same filar: this happens if and only if the multiplicities $n_3^{(1)}$ and $n_3^{(2)}$ are equal, or, equivalently, $G^{(1)}$ and $G^{(2)}$ have equal number of triangles. The lines these filars approximate are given by parametric equations

$$\begin{aligned} x &= J(1/3) + 6n_3 F_3(1/3)/n + t F_4(1/3), \\ y &= (J(2/3) - J(1/3)^2) + 6n_3 (F_3(2/3) - 2J(1/3)F_3(1/3)) / n \\ &\quad + t (F_4(2/3) - 2J(1/3)F_4(1/3)). \end{aligned}$$

The horizontal distance between two filars that contain the points corresponding to $G^{(1)}$ and $G^{(2)}$ is proportional to $n_3^{(1)} - n_3^{(2)}$ and is approximately equal to

$$6 \left(F_3(1/3) - F_4(1/3) \frac{F_3(2/3) - 2J(1/3)F_3(1/3)}{F_4(2/3) - 2J(1/3)F_4(1/3)} \right) \frac{n_3^{(1)} - n_3^{(2)}}{n}.$$

For $n = 12, 14, 16, 18$ the approximate horizontal distances between the neighboring filars are 0.00181, 0.00155, 0.00136, 0.00121 respectively. As one can easily see on Figure 1, filars actually get closer to each other as n gets larger in proportion with $1/n$. However, the slope of filars is independent of n and is equal to $F_4(2/3)/F_4(1/3) - 2J(1/3) \approx 15.89$. All the above agree perfectly with the numerical data plotted in Figures 1 and 2.

Each filar splits into subfilars labelled by the number n_4 of quadrangles in the corresponding graphs. These subfilars approximate line segments of slope $F_5(2/3)/F_5(1/3) - 2J(1/3) \approx 33.36$. The horizontal distance between subfilars is measured by increments of

$$\frac{8}{n} \left(F_4(1/3) - F_5(1/3) \frac{F_4(2/3) - 2J(1/3)F_4(1/3)}{F_5(2/3) - 2J(1/3)F_5(1/3)} \right).$$

One can pursue this kind of analysis for subfilars of any level (or depth).

Finally, a comment is in order. The first one concerns the number of filars, or, equivalently, how many distinct values the multiplicity m_3 (= the number of triangles) can attain for a regular graph on n vertices. We sketch an argument that gives an upper bound for m_3 in terms of n . It can be shown that the maximal number of triangles is achieved in planar graphs. By the Euler characteristic formula we have $v - e + f = 2$, where v, e, f are the numbers of vertices, edges and faces of a planar graph. Denote by f_k the number of its k -gonal faces. Then, for a d -regular graph on n vertices $v = n$, $e = nd/2$, $f = \sum f_k$.

Substituting these expressions into the Euler characteristic formula, we get

$$\left(1 - \frac{d}{2}\right)n + \sum_{k \geq 3} f_k = 2.$$

Say, for $d = 3$ a careful analysis of this formula shows that $m_3 = f_3 \leq 2\lfloor n/4 \rfloor$ with the exception of K_4 , the complete graph on 4 vertices. This upper bound is sharp. For n divisible by 4 it is achieved by looping a *string of diamonds* shown in Figure 5(a)(cf. [3], [5]). When $n \equiv 2 \pmod{4}$, we need to attach a *clasp* on either end of a string of diamonds, as shown in Figure 5(b). In fact, for cubic graphs on $n \geq 8$ vertices the multiplicity m_3 can be any number between 0 and $2\lfloor n/4 \rfloor$; the corresponding examples can also be easily constructed (e.g. $m_3 = 0$ for bipartite graphs).

Appendix. The Ihara-Selberg trace formula

The famous Selberg trace formula relates the eigenvalue spectrum of the Laplace operator on a hyperbolic surface to its length spectrum – the collection of lengths of closed geodesics counted with multiplicities. An immediate consequence of the Selberg trace formula is that the eigenvalue spectrum and the length spectrum uniquely determine one another. A similar result is valid for regular graphs [4], [1]. To formulate it precisely we need to introduce some terminology.

We consider oriented closed paths in graphs up to cyclic permutations of vertices. An elementary homotopy is a transformation of a closed path of the form

$$(v_1, \dots, v_j, \dots, v_n, v_1) \mapsto (v_1, \dots, v_j, v', v_j, \dots, v_n, v_1),$$

where v_j and v' are adjacent vertices. Two closed paths are called (freely) homotopic if one can be transformed into another by a sequence of elementary homotopies or their inverses. The unique shortest representative in a (free) homotopy class of closed paths is called a *closed geodesic*. The *length* $\ell(\gamma)$ of a closed geodesic γ is the number of edges it contains; γ is called *primitive* if it is not a power of a shorter geodesic.

Now let G be a regular graph of degree $d = q + 1$ on n vertices. Denote by A its adjacency matrix, and let $\{\lambda_1 > \lambda_2 \geq \dots \lambda_n\}$ be the spectrum of A . Note that $\lambda_1 = q + 1$ and $|\lambda_i| \leq q + 1$. The following result can be found in [1]:

Theorem 1. *Let $h : \mathbb{Z} \rightarrow \mathbb{C}$ be a sequence of complex numbers such that $h(n) = h(-n)$ for all $n \in \mathbb{Z}$ and*

$$\sum_{n=1}^{\infty} |h(n)|q^{n/2} < \infty.$$

Put $\hat{h}(z) = \sum_{n=-\infty}^{\infty} h(n)z^{-n}$, the discrete Fourier transform of $h(n)$. Then

$$\sum_{i=1}^n \hat{h}(z_i) = \frac{nq}{2\pi\sqrt{-1}} \oint_{|z|=1} \hat{h}(z) \frac{1-z^2}{q-z^2} \frac{dz}{z} + \sum_{\gamma} \sum_{k=1}^{\infty} \frac{\ell(\gamma)}{q^{n\ell(\gamma)/2}} h(k\ell(\gamma)), \quad (7)$$

where z_i is related to λ_i by the equation $\lambda_i = \sqrt{q}(z_i + z_i^{-1})$, and γ runs over the set of all primitive closed geodesics in G .

Formula (1) follows from (7) if we take $h(n) = I_n(2\sqrt{qt})$. Then we have $\hat{h}(z) = e^{t\sqrt{q}(z+z^{-1})}$. The integrals that enter (1) and (7) are related to each other by the change of variable $s = \sqrt{q}(z + z^{-1})$.

Acknowledgements. We are indebted to Jessica Nelson and Wayne Lobb for some help with the initial numerical experiments as well as for a number of discussions, and to Markus Meringer for his help with GENREG. The work of VE, JF and SL was supported, in part, by the Australian Research Council Discovery grant DP0666632. While this work was done, SL was at the University of South Australia. The work of PZ was partially supported by the President of Russian Federation grant NSh-U329.2006.1 and by the Russian Foundation for Basic Research grant 05-01-00899.

References

1. Ahumada, G.: Fonctions périodique et formule des traces de Selberg sur les arbres, C. R. Acad. Sci. Paris 305, 709–712 (1987).
2. Bollobás, B.: Modern Graph Theory, New York: Springer Verlag (1998).
3. Greenlaw, R., Petreschi, R.: Cubic graphs. ACM Comput. Surv. 27, 471–495 (1995).
4. Ihara, Y. On discrete subgroup of the two by two projective linear group over p-adic field, J. math. Soc. Japan 18:3 (1996).
5. Korfhage, R.R.: Discrete Computational Structures, 2nd ed., New York: Academic Press (1984).
6. Meringer, M.: Fast generation of regular graphs and construction of cages. J. Graph Th. 30, 137–146 (1999).
7. Mnëv, P.: Discrete path integral approach to the trace formula for regular graphs, ArXiv:math-ph/0609028, (2006).
8. Selberg, A.: Harmonic analysis and discontinuous groups in weakly symmetric Riemannian spaces with application to Dirichlet series, J. of the Indian Math. Soc. 20. 47–82, (1956).
9. Watson, G. N.: A Treatise on the Theory of Bessel Functions, Second Edition, Cambridge University Press (1966).

Received: September, 2006

A fractal structure of cubic graphs

V. Ejov¹, J.A. Filar¹, S.K. Lucas¹

School of Mathematics and Statistics, University of South Australia, Mawson Lakes SA 5095 AUSTRALIA

Abstract. In this note we exhibit a characteristic structure of the class of all cubic graphs that stems from the spectral properties of their adjacency matrices. Since the structure appears to be novel and has a fractal threadlike appearance, we call it the multifilar structure. We provide an algebraic explanation of this structure.

Key words. Cubic graph, fractal, eigenvalues

1. A numerical experiment

Consider the set of all regular cubic graphs with n vertices, which can be conveniently enumerated using the GENREG program of Markus Meringer [4]. Each graph has an associated adjacency matrix, and so a set of eigenvalues for each graph can be found numerically. In the interests of statistical analysis, we might want to take the means and variances of each set of eigenvalues. However, since the diagonal entries of the adjacency matrices are zero (no loops), the eigenvalues sum to zero. In the interests of producing results with some variation, and originally motivated by solving systems of linear first order differential equations, we take the exponential of the eigenvalues before finding their mean and variance. As a final modification, this time motivated by the authors' interest in Markov processes, we replace the adjacency matrix A by the related doubly stochastic matrix $\frac{1}{3}A$. The theory of Markov chains then states that the probability of being at the j th vertex after a walk of length i in the graph with each edge equally likely to be chosen is the j th element of the vector $(\frac{1}{3}A)^i \mathbf{x}$, where the k th element of the vector \mathbf{x} is the probability of starting at the k th vertex.

In summary, we follow the following procedure. Given an (even) number of vertices n , find the adjacency matrices of all regular cubic graphs. In each case, divide the adjacency matrix by three, find its eigenvalues, take their exponential, and then find their mean and variance. Each cubic graph is then represented by a single dot on a plot of mean versus variance. Figure 1 shows the results of applying this procedure with $n = 8, 10, 12, 14, 16, 18$, where the number of regular cubic graphs in each case is 5, 19, 85, 509, 4060, 41301 respectively. There appears to be a very definite structure in these plots. In each case the data appear in distinct groups that at this scale seem to be straight lines with roughly the

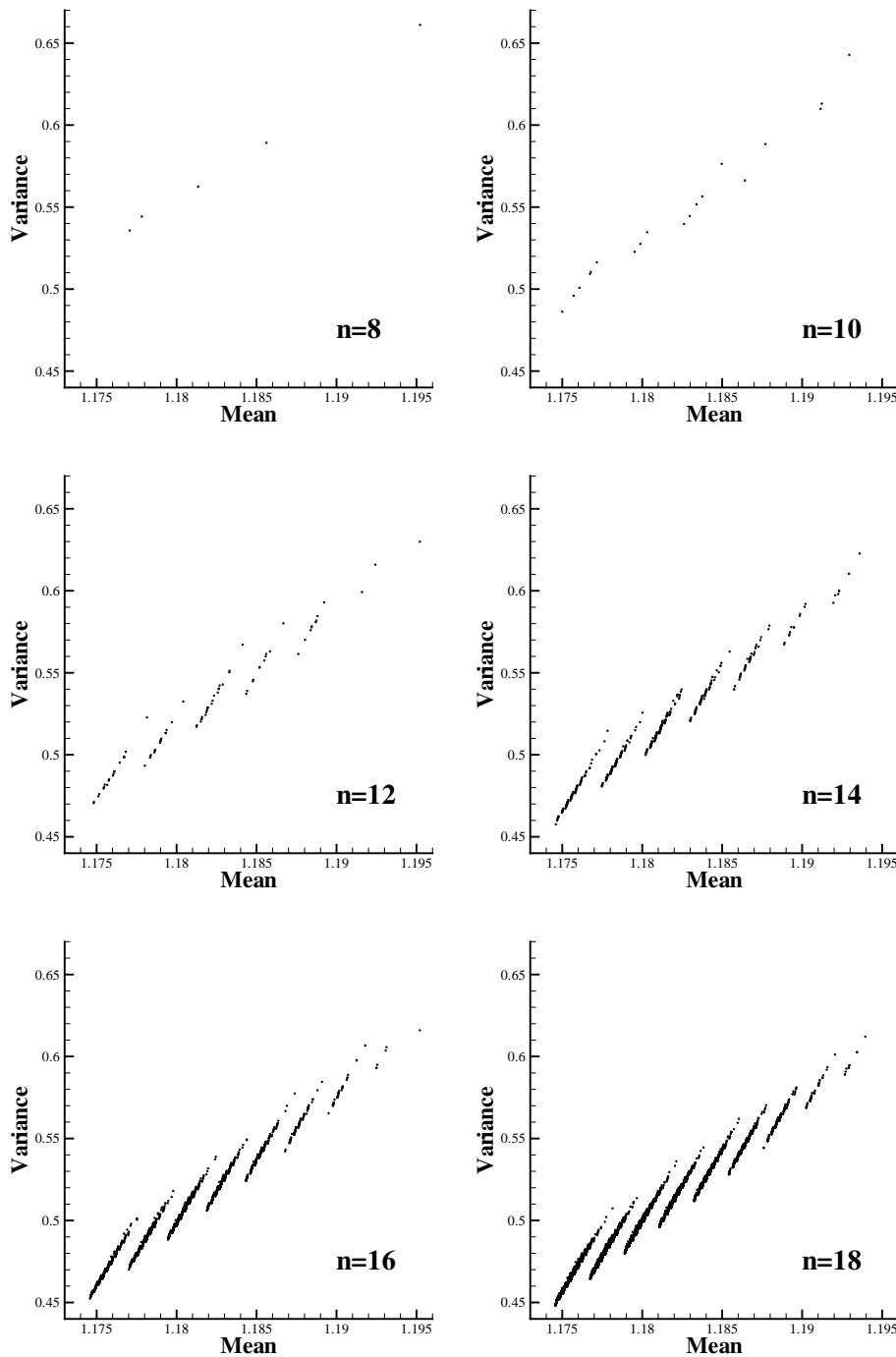


Fig. 1. Plots of mean versus variance for the exponential of the eigenvalues of the doubly stochastic matrices induced by all regular cubic graphs with various numbers of vertices.

same slope and distance separating them. Due to their form, we would like to name these groups “filars”, whose dictionary meaning is “threadlike”¹.

An even greater level of structure exists within each filar. Figure 2(a) repeats the results for $n = 16$, and Figure 2(b) zooms in on the leftmost filar. We can see that each filar is in fact made up of smaller groups of approximately straight lines, all roughly parallel and

¹ The name also recognizes the second author’s initial investigation of these features.

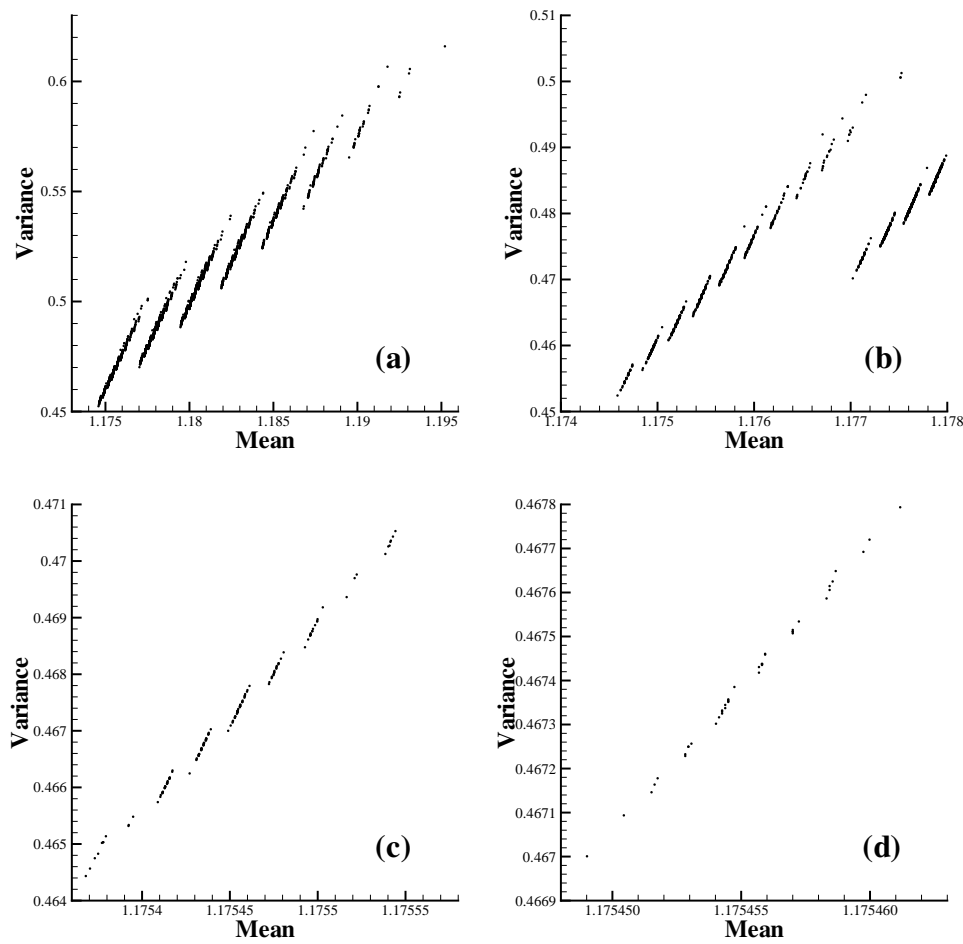


Fig. 2. Successively zooming in on the $n = 14$ plot

the same distance apart, with a higher slope than the original. We shall call each of these groups a sub-filar, and Figure 2(c) zooms in on the fourth sub-filar from the left in Figure 2(b). The structure continues in Figure 2(d), which zooms in on the 5th sub-subfilar of Figure 2(c). Since a fractal is defined as a self-similar image, where the same structure is evident when magnifying one part of the image, we see that these figures appear to be a fractal. The larger the number of vertices, the more levels of magnification can be undertaken before the number of data points becomes small enough for the self-similar structure to be lost. Collectively, we refer to this phenomenon as the “multifilar structure” of cubic graphs.

Finally, it is worth noting that this behavior is not limited to cubic graphs. Plots for quartic graphs (every vertex of degree four) show exactly the same structure. However, we note that cubic graphs in a certain sense are the generic regular graphs (e.g. Greenlaw and Petreschi [2]).

Having – to the best of our knowledge – for the first time discovered this property of cubic graphs, the aim of the following section is to theoretically explain the structure of a filar.

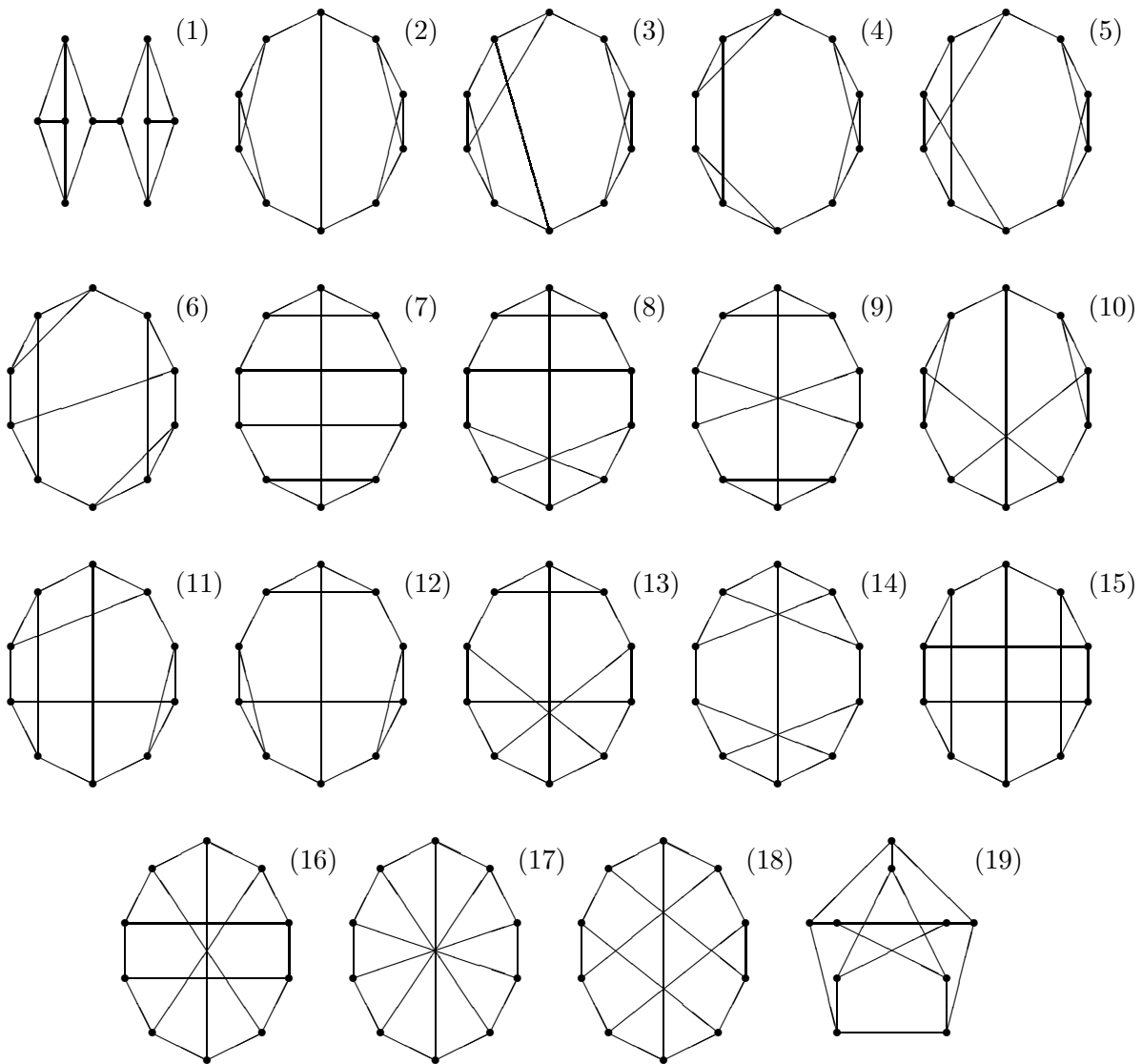


Fig. 3. All cubic graphs with ten vertices, as output by GENREG

2. Theoretical Justification

2.1. Ten vertex cubic graphs in detail

Before developing any theory, it is instructive to consider the case $n = 10$ in detail. Figure 3 shows all 19 regular cubic graphs with ten vertices, labelled in the order produced by GENREG, and Figure 4 repeats Figure 1(b), but with labels on the data points indicating graph number. We can see a pattern in terms of which graphs are in each filar. Graphs 19,18,16,17,15,14 in the first (leftmost) filar have no subcycles of length 3, which we shall call triangles from now on. Graphs 13,11,8 in the second filar have exactly one triangle, graphs 10,9,6,7,5 in the third filar have exactly two triangles, graphs 12,3 in the fourth filar have exactly three triangles, and graphs 4,2,1 in the fifth filar have exactly four triangles. Note that each triangle is equivalent to 6 closed walks of length 3 – 3 possible starting vertices, and two possible traversal directions. Concentrating on the first filar, graphs 19,18,16,17,15,14 have exactly 0,2,3,5,5,6 subcycles of length 4 respectively. Special

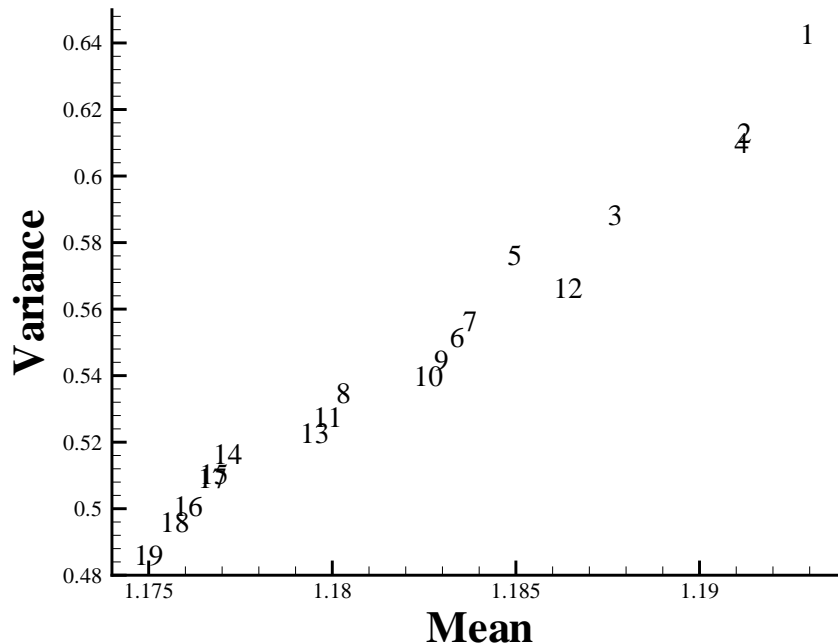


Fig. 4. A reproduction of Figure 1 ($n = 10$) with labels replacing data points related to associated with graphs in Figure 3

emphasis should be given to the data points for graphs 17 and 15. They are extremely close together, and have the same number of subcycles of lengths 3 and 4 (0 and 5 respectively). They only vary in number of subcycles of length 5, numbering 0 and 2. Similarly, graphs 4 and 2 both have four 3-subcycles, two 4-subcycles, and only vary in the number of 5-subcycles (two and four). These results suggest that membership in a filar structure is related to the number of subcycles of various lengths in the original graph – although this does not explain why filars approximate straight lines.

2.2. Preliminary results

A well-known result from undergraduate linear algebra states that the trace of the matrix A (the sum of its main diagonal) equals the sum of its eigenvalues λ_i . More generally,

$$\text{tr}(A^j) = \sum_{i=1}^n \lambda_i^j, \quad (1)$$

for any nonnegative integer j . This is a compelling starting point, since when A is the adjacency matrix of a graph, the (k, k) th element of A^j represents the number of closed walks starting and finishing at vertex k of length j . While we were able to identify numbers of subcycles in Figure 3 and their relationship to the plot in Figure 4, the number of closed walks is closely related to the number of subcycles.

Additionally, since the matrix A represents an undirected graph, it is symmetric, and its eigenvalues are real. We can assume that its eigenvalues are ordered in magnitude as $|\lambda_1| \geq |\lambda_2| \geq \dots \geq |\lambda_n|$. A number of other results on the eigenvalues of the adjacency

matrix of a graph can be found in section VIII.2 of Bollobás [1]. In particular, for a cubic graph, $\lambda_1 = 3$ and is an eigenvalue of multiplicity one. If $\lambda_2 = -3$ is also an eigenvalue, then the graph must be bipartite, and every eigenvalue λ has a matching eigenvalue $-\lambda$.

We can also make some statements about the number of closed walks of various lengths in a cubic graph. All cubic graphs have 0 and $3n$ closed walks of length 1 and 2 respectively, so

$$\text{tr}(A^0) = n, \quad \text{tr}(A^1) = 0 \quad \text{and} \quad \text{tr}(A^2) = 3n. \quad (2)$$

In addition (for non-bipartite graphs) using (1),

$$\text{tr}((A/3)^j) - 1 = \sum_{i=2}^n \lambda_i^j, \quad (3)$$

where we have moved the largest eigenvalue to the left hand side, and so $\text{tr}((A/3)^j) \rightarrow 1$ in the limit $j \rightarrow \infty$, and $|\text{tr}((A/3)^j) - 1|$ is a strictly decreasing sequence in j for $j \geq 2$. The rate of approach is dominated by the magnitude of λ_2 – a smaller value increases the rate of convergence. Depending on the signs of the various eigenvalues, $\text{tr}((A/3)^j)$ may be < 1 for odd j (although always nonnegative), but will certainly be > 1 for even j . Thus $\text{tr}((A/3)^j)$ is typically converging to 1, with a rate dependent on the magnitude of λ_2 , in an oscillatory manner. Note that if the (cubic) graph is bipartite, $\lambda_2 = -3$, and $\text{tr}((A/3)^j) = 0$ for all odd j since there are no closed walks of odd length in a bipartite graph, and as $j \rightarrow \infty$, $\text{tr}((A/3)^j) \rightarrow 2$. Since $\lambda_2 = -3$, the rate of converge depends on the magnitude of λ_3 .

Finally, we will be interested in the number of triangles in a cubic graph. For a bipartite graph, the lower limit of zero is achieved. An upper limit is implicit in Greenlaw and Petreschi [2], which we make explicit here. The only way a node in a cubic graph can be a member of three triangles is in the complete graph K_4 , a very limited case. For a node to be a member of two triangles requires the structure in figure 5(a), which is called a *diamond*. For a node to be in either one or zero triangles requires the structure in figures 5(b) and (c). A *string of diamonds* is a number of diamonds linked together as in figure 5(d), and if the string loops around and joins onto itself, it is called a *ring of diamonds*. Now if we let a , b and c be the number of nodes in a cubic graph in two, one and zero triangles respectively, Korfhage [3] showed that

$$a = 2k_1, \quad b = a + 3k_2, \quad \text{and} \quad n = a + b + c, \quad (4)$$

where k_1 and k_2 are nonnegative integers. Since the number of triangles in a cubic graph is $(2a + b)/3$, some straightforward algebra shows that this is maximized when $b = a$ and $c = 0$, which is in fact the case of a ring of diamonds. This only occurs when n is divisible by 4. If $\text{mod}(n, 4) = 2$, we cannot improve upon the number of triangles, and need to set $c = 2$. This is equivalent to putting a *clasp* on either end of a string of diamonds, as shown in figure 5(e). Thus, the maximum number of triangles in a graph is $2\lfloor n/4 \rfloor$, and so $\text{tr}(A^3) \leq 3n$, since there are six closed walks of length three associated with each triangle.

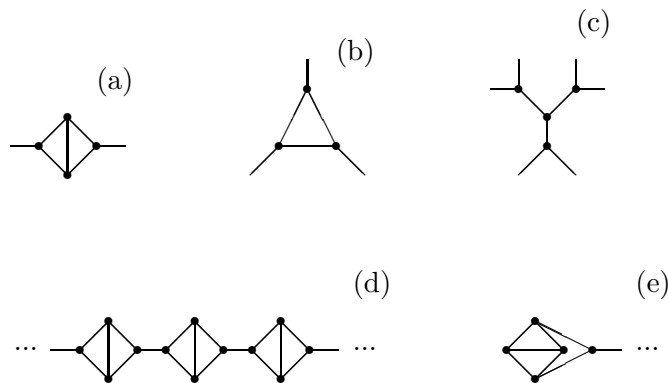


Fig. 5. Nodes on (a) two, (b) one and (c) zero triangles, (d) a string of diamonds and (e) a clasp

2.3. Clustering into filars

To explain the separation of graphs into filars, the mean of the exponential of the eigenvalues of $\frac{1}{3}A$ can be written as

$$\mu = \frac{1}{n} \sum_{i=1}^n \exp(\lambda_i) = \frac{1}{n} \sum_{i=1}^n \sum_{j=0}^{\infty} \frac{\lambda_i^j}{j!} = \frac{1}{n} \sum_{j=0}^{\infty} \frac{1}{j!} \sum_{i=1}^n \lambda_i^j = \frac{1}{n} \sum_{j=0}^{\infty} \frac{\text{tr}(A^j)}{3^j j!}, \quad (5)$$

where we have used the result $\text{tr}((A/m)^j) = \text{tr}(A^j)/m^j$. Thus, the mean of the exponential of the eigenvalues is the sum of the number of closed walks of length j scaled by $3^j j!$. Using (2), (5) can be rewritten as

$$\mu = \frac{7}{6} + \frac{1}{n} \sum_{j=3}^{\infty} \frac{\text{tr}(A^j)}{3^j j!}. \quad (6)$$

Now the result on the number of triangles in a cubic graph tells us that $\text{tr}((A/3)^j)/n < 3/27$. Combined with the decreasing nature of $\text{tr}((A/3)^j)$ and the factorial in the denominator, we see that each term in the sum of (6) becomes increasingly small. Two graphs whose number of closed walks differ for the first time for walks of length k will have μ values whose difference becomes smaller as k increases. This is analogous to the decimal representation of reals, where two reals are increasingly close together as the number of identical digits up to length k increases. The only difference is replacing the scaling factor 10^{-k} by $1/k!$. Therefore, two graphs with the same number of closed walks of length three will be in the same filar. The difference in the number of closed walks of length four identifies their positions within the filar, due to the $1/4!$ term. Note that graphs in adjacent filars can have overlapping values of μ , when the number of walks of length 4 are at extremes. Thus (6) explains much of the structure of filars in Figure 1. All values of μ are slightly larger than $7/6$, and graphs will be in different filars if the number of closed walks of length three (which equal the number of subcycles of length 3) are different. Within a given filar, numbers of closed walks of length 4 identify which subfilar a given graph lies within, and so on using closed walks of increasing length to produce the fractal structure of a filar.

At this point it is appropriate to comment on the influence of the factor $1/3$ when scaling the adjacency matrix of a graph. If a scale greater than $1/3$ is used, then the trace of the matrix will grow as the power increases. If we work with the original adjacency matrix (scaling factor 1), then variations between graphs at different lengths of walks are not differentiated, and there is no discernable pattern in the plots of mean versus variance of the exponential of the eigenvalues. If, however, we use a scaling factor less than $1/3$, then variations in m between graphs due to differences in closed walk lengths becomes more exaggerated. For example, with a scaling factor of $1/100$, the filars collapse into what are essentially separated dots associated with the number of subcycles of length 3. Variations due to closed walks of length greater than three equate to variations in m too small to see on a plot.

2.4. Straight line shape of filars

While the previous subsection explains the multifilar structure, further analysis is required to explain their appearance as straight lines of different slope depending on what level within the substructure we are observing. We will need an expression for the variance, which is

$$\begin{aligned}
s^2 &= \frac{1}{n-1} \sum_{i=1}^n (e^{\lambda_i} - \mu)^2 = \frac{1}{n-1} \sum_{i=1}^n (e^{2\lambda_i} - 2\mu e^{\lambda_i} + \mu^2) \\
&= \frac{1}{n-1} \sum_{i=1}^n \left(\sum_{j=0}^{\infty} \frac{(2\lambda_i)^j}{j!} - 2\mu \sum_{j=0}^{\infty} \frac{\lambda_i^j}{j!} + \mu^2 \right) \\
&= \frac{1}{n-1} \left(\sum_{j=0}^{\infty} \left(\frac{1}{j!} \sum_{i=1}^n (2\lambda_i)^j \right) - 2\mu \sum_{j=0}^{\infty} \left(\frac{1}{j!} \sum_{i=1}^n \lambda_i^j \right) + n\mu^2 \right) \\
&= \frac{1}{n-1} \left(\sum_{j=0}^{\infty} \frac{\text{tr}((2A)^j)}{3^j j!} - 2\mu \sum_{j=0}^{\infty} \frac{\text{tr}(A^j)}{3^j j!} + n\mu^2 \right) \\
&= \frac{1}{n-1} \left(\sum_{j=0}^{\infty} \frac{2^j \text{tr}(A^j)}{3^j j!} - n\mu^2 \right),
\end{aligned} \tag{7}$$

using (5) and the fact that $\text{tr}(2^j A^j) = 2^j \text{tr}(A^j)$.

Now assume that we move from a graph A with mean μ_A to another graph B with mean μ_B where $\text{tr}(B^j) = \text{tr}(A^j)$ for all $j \neq k$ and $\text{tr}(B^k) = \text{tr}(A^k) + \delta$. The variable δ represents the difference in the number of closed walks of length k between the two graphs. Now this initially may seem unrealistic since the graphs A and B will almost always also have different numbers of closed walks of lengths greater than k . However, our previous analysis shows that combining the factorial in the denominator with the bounded behaviour of traces of $A/3$ means that changes at lower levels will make relatively small contributions to the mean and variance, and so can be ignored to a first approximation. We have that

$$\mu_B = \mu_A + \frac{\delta}{n3^k k!} \quad \text{and} \quad \mu_B^2 = \mu_A^2 + \frac{2\delta\mu_A}{n3^k k!} + \frac{\delta^2}{n^2 3^{2k} (k!)^2}, \tag{8}$$

and it follows from (7) that

$$s_B^2 = s_A^2 + \frac{\delta 2^k}{(n-1)3^k k!} - \frac{2\delta\mu_A}{(n-1)3^k k!} - \frac{\delta^2}{n(n-1)3^{2k} (k!)^2}. \tag{9}$$

Since $\delta^2/(n^2 3^{2k} (k!)^2)$ is negligible compared to other terms, this indicates that when moving from graphs A to B , μ increases by $\delta/(n 3^k k!)$ and s^2 increases by $\delta(2^k - 2\mu)/((n-1)3^k k!)$. Since μ only changes over a very small range for the graphs in question, we have that the increases in both μ and s^2 are linear in δ , with ratio (s^2 increase/ μ increase) equal to $(n/(n-1))(2^k - 2\mu)$. This explains why filars are roughly straight lines, with varying slopes as you zoom in on the subfilar structure. Graphs with the same traces up to a given power will be in a subfilar with a slope depending on the level of similarity of the graphs.

Finally, a comparison with the actual lines of best fit to the various filars in Figures 1 and 2 show that the above slope is a slight overestimate. This can be explained by realizing that changing the number of closed walks of length k in a graph will inevitably change the number of closed walks of longer length. Perturbations due to these additional variations, however, are of second order.

Acknowledgements. We are indebted to Jessica Nelson and Wayne Lobb for some help with the initial numerical experiments as well as for a number of discussions, and to Markus Meringer for his help with GENREG. This work was supported, in part, by an Australian Research Council (Discovery) grant.

References

1. Bollobás, B.: Modern Graph Theory, New York: Springer Verlag 1998
2. Greenlaw, R., Petreschi, R.: Cubic graphs. ACM Comput. Surv. 27, 471–495 (1995)
3. Korfhage, R.R.: Discrete Computational Structures, 2nd ed., New York: Academic Press 1984
4. Meringer, M.: Fast generation of regular graphs and construction of cages. J. Graph Th. 30, 137–146 (1999)

Received: August, 2005